# Simultaneous displacement measurement method of multiple targets based on laser self-mixing interference*

**ZHAO Yan** (赵岩)[1,2]**, **ZHANG Ai-ling** (张爱玲)[1,3], and **ZHANG Hai-wei** (张海伟)[1,3]

*1. School of Electrical and Electronic Engineering, Tianjin University of Technology, Tianjin 300384, China*

*2. Tianjin Key Laboratory for Control Theory and Applications in Complicated Systems, Tianjin 300384, China*

*3. Tianjin Key Laboratory of Film Electronic and Communication Device, Tianjin 300384, China*

(Received 28 February 2020; Revised 4 May 2020)



In order to simultaneously measure the displacements of multiple targets, the laser self-mixing interference (SMI) measurement method based on variational mode decomposition (VMD) is proposed. The SMI signal containing the motion information of the external targets is detected by a photodiode. The VMD can non-recursively decompose the mixed SMI signal into SMI signals corresponding to different external targets. The displacement signals can be reconstructed by fringe counting method and interpolation method. The experimental results show that the displacement signals of different external targets can be reconstructed with half wavelength accuracy, which verifies the correctness and feasibility of this method. This method can improve the measurement efficiency, which offers an effective method for the multi-channel displacement measurement.

**Document code:** A **Article ID:** 1673-1905(2021)03-0165-5

**DOI** https://doi.org/10.1007/s11801-021-0034-5

In modern manufacturing industry, it is often necessary to measure the displacements of targets at the same time. The multi-target displacement measurement methods include laser interference[1], laser diffraction[2], laser collimation[3]. In recent years, the laser self-mixing interference (SMI) technology has been applied to multi-target displacement measurement. When a part of the light emitted by the laser is reflected from the external target and re-entered into the active laser cavity, the SMI phenomenon will occur[4-6].

According to the intensity of optical feedback, the level of optical feedback can be divided into: weak feedback, moderate feedback and strong feedback[7]. In the strong feedback regime, there will be nonlinear effect and the SMI signal will enter into chaos state. In order to avoid the nonlinear effect caused by the optical feedback, the level of optical feedback is limited to weak feedback or moderate feedback by controlling the driving current.

In recent years, the SMI model with multiple external targets has been studied[8-13]. The SMI system with two external cavities is designed to improve the measurement sensitivity[10]. The Lang-Kobayashi equations are modified to analyze the sensing performance with the LD in the period-one oscillation state. The SMI system with a single laser diode is used to simultaneously measure the displacements of both ablation front and target during laser percussion drilling micromachining[11]. The Lang-Kobayashi model was extended in order to interpret the experimental results. The theoretical analysis is in good agreement with the experimental result. The dual-channel self-mixing displacement measurement system in a linear cavity fiber laser is proposed[12]. The theoretical model based on the three-cavity is analyzed and the experimental results show that the different movement of each channel can be detected by the dual-channel linear cavity fiber laser SMI system. The two-external-cavity SMI system with a semiconductor laser is investigated and analyzed[13]. The simulation and experimental results show that the mixed SMI signal of two-external-cavity feedback is similar to the superposition of the two SMI signals.

The signal separation methods mainly include empirical mode decomposition (EMD)[14], ensemble empirical mode decomposition (EEMD)[15], variational mode decomposition (VMD)[16,17]. According to the time-scale features of the signal, EMD can adaptively decompose the signal into several intrinsic mode functions (IMFs) from high frequency to low frequency. EEMD can adaptively decompose the signal into several IMFs by using white noise to smooth the abnormal incident in the signal and eliminate the influence of white noise with multiple mean method. VMD can adaptively decompose any signal into an ensemble of band-limited intrinsic mode functions, where their center frequencies are estimated

* This work has been supported by the National Natural Science Foundation of China (No.61803281), the Tianjin Natural Science Foundation (Nos.18JCQNJC75500 and 18JCQNJC71200), and the Scientific Research Project of Tianjin Education Commission (Nos.2017KJ253 and 2018KJ136).

** E-mail: tjut_eric@163.com

on-line and all modes are extracted concurrently. Compared with EMD and EEMD, the VMD algorithm is more robust to noise because of the Wiener filtering embedded to update the mode directly in Fourier domain. This paper attempts to apply VMD to SMI signals, which is an extension of VMD theory and a supplement to SMI signal separation technology.

The displacement measurement methods based on SMI include fringe counting[18], phase measurement method[19], phase unwrapping[20]. Similar to the traditional laser interference, each interference fringe of SMI signal corresponds to the displacement change of half wavelength of the external target. Therefore, the displacement of a target can be measured by calculating the number of interference fringes. By combining the interpolation method with the fringe counting method, the displacement can be measured conveniently and accurately.

In this paper, the SMI measurement method of multi-target displacement based on VMD is proposed. VMD can separate the mixed SMI signal adaptively, so as to ensure the accuracy of displacement measurement. The displacement measurement method based on VMD is illustrated and the performance of VMD algorithm is analyzed. The displacement measurement system with a single SMI sensor is set up to verify the feasibility and effectiveness of the proposed method.

The schematic diagram of SMI system with two external targets is shown in Fig.1. The laser beam emitted by the LD is divided into two beams by the beam splitter. The two beams are reflected by the vibration targets respectively and re-enter the laser active cavity. The feedback light coherently interferes with the optical field inside the laser cavity and modulates the output power of the laser.

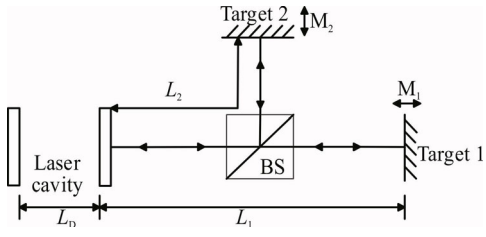


**Fig.1 Schematic diagram of SMI system with two external targets**

The theory model of SMI system with two external targets is described as follows[11-13]:

$$\omega_0\tau_D = \omega\tau_D + C_1\sin\left[\omega\tau_1 + \arctan\alpha\right] + C_2\sin\left[\omega\tau_2 + \arctan\alpha\right], \quad (1)$$

$$P = P_0\left[1 + m_1\cos\left(\omega\tau_1\right) + m_2\cos\left(\omega\tau_2\right)\right], \quad (2)$$

$$L_1(t) = \frac{\lambda_0\omega\tau_1}{4\pi}, \quad (3)$$

$$L_2(t) = \frac{\lambda_0\omega\tau_2}{4\pi}, \quad (4)$$

where $C_1$ and $C_2$ are the optical feedback level factors, $\alpha$ is the laser linewidth enhancement factor, $m_1$ and $m_2$ are the modulation indexes, $P$ and $P_0$ represent the laser power with and without optical feedback respectively, $L_1$ and $L_2$ are the external cavity lengths between the laser exit facet and the two targets, $\tau_i$=2$L_i$/$c$ ($i$=1,2) is the round-trip delay time determined by the external cavity length and the speed of light, $\tau_D$ is the round-trip delay time inside the laser cavity, and $\lambda_0$ is the laser wavelength without optical feedback.

The principle of displacement measurement of multiple external targets is shown in Fig.2. Firstly, the mixed SMI signal is decomposed into two SMI signals corresponding to the external targets by VMD algorithm. The fringe counting method is used to estimate the displacement roughly and the interpolation method is used to smooth the displacement, so that the displacement signal of each external target can be obtained.

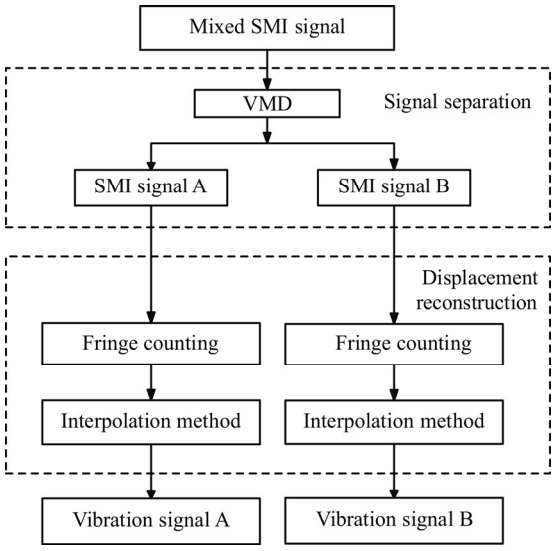


**Fig.2 Schematic diagram of the proposed displacement measurement method**

VMD can decompose a multi-component signal into several intrinsic mode functions (IMFs) and the IMF is defined as follows[16]:

$$u_k(t)=A_k(t)\cos(\phi_k(t)), \quad (5)$$

where $A_k(t)$ is the envelope signal, $\phi_k(t)$ is the instantaneous phase, and $k$ is the serial number of IMF.

The real valued signal $f$ is decomposed into a discrete number of sub-signals $u_k$ by VMD. Each IMF is compact around a center pulsation $\omega_k$ and its bandwidth is estimated by $H^1$ Gaussian smoothness of the shifted signal.

$$\min_{\{u_k\},\{\omega_k\}}\left\{\sum_k\left\|\partial_t\left[\left(\delta(t)+\frac{j}{\pi t}\right)\times u_k(t)\right]e^{-j\omega_k t}\right\|_2^2\right\},$$
$$\text{s.t.}\sum_k u_k = f, \quad (6)$$

where $\{\omega_k\}=\{\omega_1,\ldots,\omega_K\}$ denotes the frequency center of each component, and $\{u_k\}=\{u_1,\ldots,u_K\}$ denotes $K$ IMF components.

By introducing the extended Lagrange, the constrained variational problem is transformed into a non-constrained variational problem and its expression is as follows[16]:

$$L\left(\{u_k\},\{\omega_k\},\gamma\right)=$$
$$\beta\sum_k\left\|\partial_t\left[\left(\delta(t)+\frac{\mathrm{j}}{\pi t}\right)\times u_k(t)\right]\mathrm{e}^{-\mathrm{j}\omega_k t}\right\|_2^2+$$
$$\left\|f(t)-\sum_k u_k(t)\right\|_2^2+\left\langle\gamma(t),f(t)-\sum_k u_k(t)\right\rangle, \quad (7)$$

where $\beta$ denotes the balancing parameter of the data-fidelity constraint, and $\gamma(t)$ denotes the Lagrange multiplier.

The update formula solved with the alternate direction method of multipliers is as follows:

$$\begin{cases}\hat{u}_k^{n+1}(\omega)=\dfrac{\hat{f}(\omega)-\sum_{i\neq k}\hat{u}_i(\omega)+\dfrac{\hat{\gamma}(\omega)}{2}}{1+2\beta(\omega-\omega_k)^2}\\ \omega_k^{n+1}=\dfrac{\int_0^\infty\omega\left|\hat{u}_k(\omega)\right|^2\mathrm{d}\omega}{\int_0^\infty\left|\hat{u}_k(\omega)\right|^2\mathrm{d}\omega}\\ \hat{\gamma}^{n+1}=\hat{\gamma}^n(\omega)+\xi\left(\hat{f}(\omega)-\sum_k\hat{u}_k^{n+1}(\omega)\right)\end{cases}, \quad (8)$$

where $n$ corresponds to the nth iteration, and $\xi$ is the update parameter.

Assuming that the external target is in sinusoidal periodic motion, the equation of motion is as follows:

$$L=L_0+\Delta L\sin\left(2\pi N f_\mathrm{t}/f_\mathrm{s}\right), \quad (9)$$

where $L_0$ is the initial distance between laser and external target, $\Delta L$ is the vibration amplitude of external target, $f_\mathrm{t}$ is the vibration frequency of external target, $f_\mathrm{s}$ is the sampling frequency, and $N$ is the number of sampling points.

According to Eqs.(1—4) and Eq.(9), the ideal SMI signals A and B with the parameters in Tab.1 can be obtained by numerical simulation. The mixed SMI signal consists of signal A and signal B and the mixed SMI signal is processed by EMD, EEMD and VMD, respectively.

**Tab.1 The parameter values of SMI simulation signals ($\lambda_0$=800 nm)**

| | $\Delta L$ | $f_\mathrm{t}$ | $f_\mathrm{s}$ | $N$ | $C$ | $\alpha$ |
|---|---|---|---|---|---|---|
| Signal A | $3\lambda_0$ | 5 Hz | 100 kHz | 20 000 | 1 | 3 |
| Signal B | $3\lambda_0$ | 60 Hz | 100 kHz | 20 000 | 1.5 | 3 |

The processing results of signal A are shown in Fig.3. We can see that the error of VMD result is the smallest and the separation effect of VMD is obviously better than that of other methods with regards to the mixed SMI signal separation. The decomposed signals B with EMD, EEMD and VMD are shown in Fig.4. We can see from the simulation results that the VMD clearly outperforms EMD and EEMD with regards to the mixed SMI signal separation.

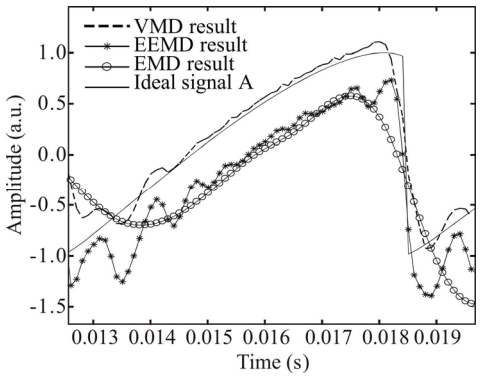


**Fig.3 Separation results of signal A by EMD, EEMD and VMD**

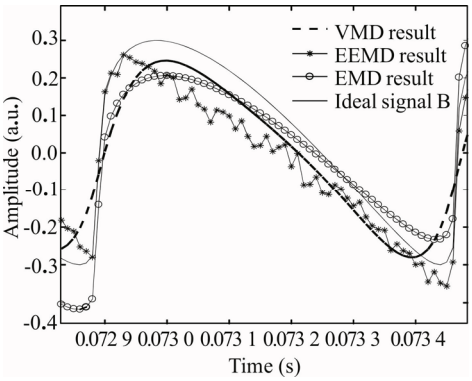


**Fig.4 Separation results of signal B by EMD, EEMD and VMD**

The experimental SMI system with two external targets is shown in Fig.5. There are two main factors influencing the measurement results: drive current stability and temperature drift. The LD with wavelength of 785 nm is biased with a dc current of 125.5 mA and the resolution of drive current is 0.01 mA. At the same time, the temperature of LD is controlled by PID algorithm and thermo electric cooler, and the temperature control accuracy is 0.002 °C. The laser beam is divided into two beams by the beam splitter, which are reflected by two piezoelectric transducers (PZT) separately. The optical attenuator can adjust the optical feedback level to weak or moderate feedback level, thus avoiding the phenomenon of fringe loss. The PZT-A and PZT-B are driven by independent control channels. The vibration frequency of PZT-A is set at 5 Hz and the peak-peak amplitude is set at 4 μm. The vibration frequency of PZT-B is set at 50 Hz and the peak-peak amplitude is set at 4 μm. The sampling frequency is 10 kHz. The mixed SMI signal is converted by current-voltage circuit, amplified and

transmitted to the oscilloscope.

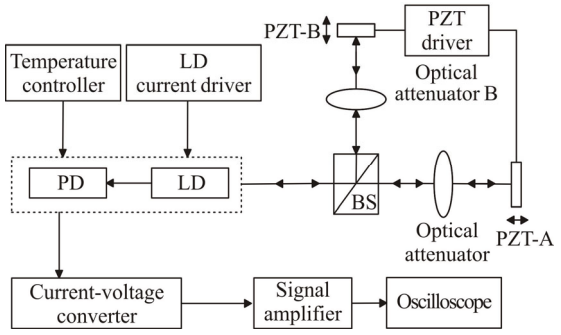


**Fig.5 Schematic diagram of experimental SMI system with two external targets**

The experimental SMI signal is shown in Fig.6(a) which contains vibration information of two external targets. The experimental result is in good agreement with the theoretical model. The experimental signal is processed by VMD and the separated SMI signals are shown in Fig.6(b) and Fig.6(c).

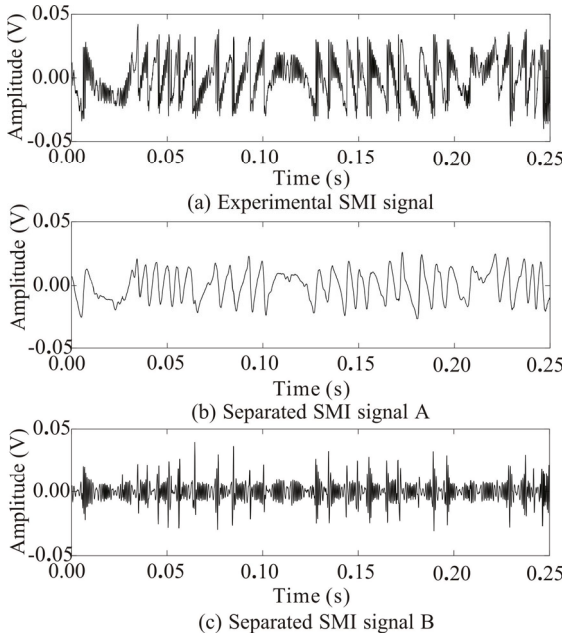


**Fig.6 VMD results of experimental SMI signal: (a) The experimental SMI signal; (b) The separated SMI signal A; (c) The separated SMI signal B**

The SMI signals A and B are processed by the fringe counting method and interpolation method[18]. The reconstructed displacements corresponding to two external targets are shown in Fig.7(a) and Fig.7(c). The errors of reconstructed displacements are shown in Fig.7(b) and Fig.7(d), where the displacement error is about $\lambda_0/2$. One reason for the measurement error is the calculation accuracy of decimal fringe. Another main reason for measurement error is that in the decomposition process, the separated SMI signal has certain distortion, which results in a certain deviation in the location of interference fringes, thus affecting the accuracy of displacement reconstruction.

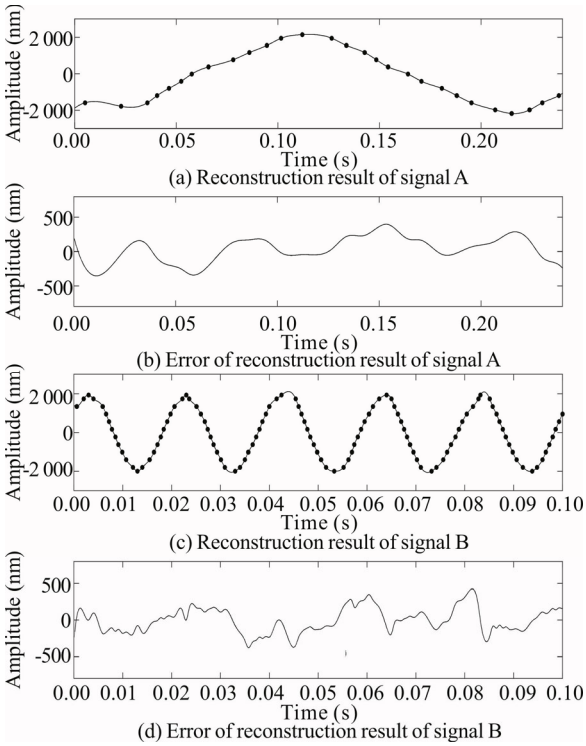


**Fig.7 Reconstruction results of experimental signal: (a) Displacement reconstruction of separated signal A; (b) Error of displacement reconstruction of separated signal A; (c) Displacement reconstruction of separated signal B; (d) Error of displacement reconstruction of separated signal B**

The average errors and standard deviation values of reconstructed displacements under different experimental conditions are shown in Tab.2. The vibration frequency of PZT-A is maintained at 5 Hz and that of PZT-B is set at 20 Hz, 40 Hz, 60 Hz, 80 Hz and 100 Hz, respectively. The optical attenuators are adjusted to realize displacement measurement under different optical feedback levels. Under different experimental conditions, the displacement measurement accuracy of two external targets can reach half wavelength, which verifies the feasibility and validity of this method.

The displacement measurement range is related to the laser power, the size of the light source and the reflectivity of the measured object surface. For the experimental system in this paper, when the measurement range is greater than 50 μm, the optical feedback level will change greatly, and the speckle effect will appear. Since the speckle effect will seriously affect the accuracy of displacement measurement, the maximum amplitude that can be measured by this method is 50 μm. According to the experimental and simulation results, when the vibration frequency ratio of two objects is 4 times to 60 times,

VMD algorithm can perform a good decomposition effect.

**Tab.2 Results of displacement reconstruction under different experimental conditions ($f_A$=5 Hz)**

| | Result of signal A | | Result of signal B | |
|---|---|---|---|---|
| | Avg. Err. (nm) | Std. Dev. (nm) | Avg. Err. (nm) | Std. Dev. (nm) |
| $f_B$=20 Hz | 37.682 6 | 133.119 1 | 55.743 1 | 171.135 7 |
| $f_B$=40 Hz | 17.427 3 | 164.288 9 | 34.269 7 | 265.900 6 |
| $f_B$=60 Hz | 39.035 0 | 87.734 0 | 36.325 4 | 209.193 1 |
| $f_B$=80 Hz | 41.263 3 | 116.981 8 | 34.484 0 | 213.429 3 |
| $f_B$=100 Hz | 57.025 1 | 165.285 2 | 33.444 3 | 262.073 5 |

The simultaneous displacement measurement method of multiple external targets based on SMI is presented and the method has no dependence on laser polarization. The SMI measurement system detects two SMI signals simultaneously by a single laser sensor. By the VMD method, two SMI signals can be effectively separated. The displacement signals can be reconstructed by fringe counting method and interpolation method. The displacement measurement accuracy is half-wavelength of the LD. This method can improve the measurement efficiency and reduce the complexity of the measurement system.

## References


[1] Chen Jia-jian, Hu Hui-zhu, Miao Li-jun, Zhou Yi-lan and Shu Xiao-wu, Optics and Precision Engineering **27**, 1435 (2019). (in Chinese)

[2] F. J. Azcona, R. Atashkhooei, S. Royo, J. M. Astudillo and A. Jha, IEEE Photonics Technology Letters **25**, 2074 (2013).

[3] Liu Li-shuang, Lv Yong, Meng Hao and Huang Jia-xing, Infrared and Laser Engineering **48**, 0617002 (2019).

[4] Zhao Yun-kun, Fan Xue-wei, Wang Chen-chen and Lu Liang, Optics and Lasers in Engineering **126**, 105866 (2020).

[5] Wang Xiu-fang, Ge Wei-jie, Chen Peng and Bi Hong-bo, Optics Communications **453**, 124383 (2019).

[6] Wang Xiu-fang, Yuan Ye, Chen Peng and Gao Bing-kun, Optical and Quantum Electronics **52**, 34 (2020).

[7] Olivier D. Bernal, Han Cheng Seat, Usman Zabit, Frédéric Surre and Thierry Bosch, IEEE Sensors Journal **16**, 7903 (2016).

[8] Ruan Yu-xi, Liu Bin, Yu Yan-guang, Xi Jiang-tao, Guo Qing-hua and Tong Jun, IEEE Photonics Journal **10**, 6804010 (2018).

[9] Niu Hai-sha, Meng Yuan-yuan, Song Jian-jun, Liu Feng and Zhu Lian-qing, Journal of Optics **21**, 125603 (2019).

[10] Ruan Yu-xi, Liu Bin, Yu Yan-guang, Xi Jiang-tao, Guo Qing-hua and Tong Jun, Applied Physics Letters **115**, 011102 (2019).

[11] F. P. Mezzapesa, L. Columbo, M. Brambilla, M. Dabbicco, A. Ancona, T. Sibillano, F. D. Lucia, P. M. Lugarà and G. Scamarcio, Optics Express **19**, 16160 (2011).

[12] Lu Liang, Zhang Wen-hua, Yang Bo, Zhou Jian-xi, Gui Hua-qiao and Yu Ben-li, IEEE Sensors Journal **13**, 4387 (2013).

[13] Chen Peng, Liu Yu-wei, Gao Bing-kun and Jiang Chun-lei, Optics Communications **410**, 693 (2018).

[14] Zhao Yi-chao and Su Yi, IEEE Transactions on Instrumentation and Measurement **69**, 929 (2020).

[15] Z. H. Wu and N. E. Huang, Advances in Adaptive Data Analysis **1**, 1 (2009).

[16] K. Dragomiretskiy and D. Zosso, IEEE Transactions on Signal Processing **62**, 531 (2014).

[17] Li Xin, Ma Zeng-qiang, Kang De and Li Xiang, Measurement **155**, 107554 (2020).

[18] S. Donati, G. Giuliani and S. Merlo, IEEE Journal of Quantum Electronics **31**, 113 (1995).

[19] Wang Ming and Lai Guan-ming, Review of Scientific Instruments **72**, 3440 (2001).

[20] C. Bes, G. Plantier and T. Bosch, IEEE Transactions on Instrumentation and Measurement **55**, 1101 (2006).